In situ resonant Raman scattering and reversible photoinduced structural change in $YBa_2Cu_3O_{6+x}$

Minoru Osada*
Advanced Materials Laboratory, National Institute for Materials Science, Tsukuba, Ibaraki 305-0044, Japan

Mikael Käll and Joakim Bäckström†
Department of Applied Physics, Chalmers University of Technology, Göteborg S412-96, Sweden

Masato Kakihana
Institute of Multidisciplinary Research for Advanced Materials, Tohoku University, Sendai 980-8577, Japan

Niels Hessel Andersen
Materials Research Department, Risø National Laboratory, DK-4000 Roskilde, Denmark

Lars Börjesson
Department of Applied Physics, Chalmers University of Technology, Göteborg S412-96, Sweden
(Received 13 September 2004; revised manuscript received 15 December 2004; published 2 June 2005)

We report on bidirectional photoswitching associated with the CuO chains in oxygen-deficient $YBa_2Cu_3O_{6+x}$ single crystals. By varying the wavelength of light polarized along the CuO chains, the material can be reversibly switched between two metastable states characterized by the existence or absence of a specific Raman scattering resonance. A comparison of the spectral efficiencies for this photoswitching with analogous data for the persistent photoconductivity and photoconductivity quenching effects suggests that the two phenomena have the same microscopic origin. We argue that the effects are due to photoinduced Cu—O charge-transfer excitations, which destabilize chains of different length depending on wavelength, and promote the growth of thermally inaccessible oxygen ordering configurations.

DOI: 10.1103/PhysRevB.71.214503 PACS number(s): 72.40.+w, 61.80.Ba, 74.25.Kc, 74.72.Bk

I. INTRODUCTION

Strongly correlated low-dimensional systems are often characterized by a mixing of charge, spin, and lattice degrees of freedom, and a rich phase diagram sensitive to external perturbations, such as magnetic field or pressure. Since high-T_c superconducting cuprates exhibit a sharp insulator-to-metal transition under carrier doping, considerable attention has been focused on the idea of modulating carrier density, and thus superconducting properties, of these materials by external perturbations. In the case of oxygen-deficient $YBa_2Cu_3O_{6+x}$ (Y123; $x=0.35-0.8$), a number of reports on persistent photoconductivity (PPC) and photoinduced superconductivity[1–3] have demonstrated that a perturbation in the form of an external photon field can have a large and permanent effect on the transport properties of a superconductor. These changes are stable after illumination at temperatures below 200 K, but thermal relaxation occurs at room temperature and can be described with a stretched-exponential, so-called Kohlrausch's law.[4] In addition in heavily oxygen-deficient Y123 ($x=0.3-0.4$), the PPC state can be *partly* quenched by near-infrared (NIR) light.[5,6]

From the beginning, it was clear that these photoinduced phenomena somehow rely on the oxygen-deficient CuO-chain layers, which contribute holes to the CuO_2 planes through photoassisted oxygen ordering[7] or electron capture at oxygen vacancies.[8] Indications of photoinduced structural modifications in the CuO chains have been found in resonance Raman scattering.[9–14] These papers consider in detail the photobleaching behavior of so-called Raman forbidden (defect-induced) modes occurring at 230/248 and 596 cm^{-1} in Y123 (Refs. 10, 12, and 13) and $RBa_2Cu_3O_{6+x}$ (R=rare earth elements)[11,14] under laser light illumination. Their intensity is maximal at $x\approx 0.7$ (Refs. 10 and 12) and a strong resonance enhancement occurs for excitation energy $\hbar\omega \approx 2.1$ eV.[9,10] It has been established that these particular phonons originate at *chain ends*, i.e., the observable as such is intimately linked to oxygen vacancies in the CuO chains.[15] The study of their intensity versus time, temperature, excitation energy, and oxygen content shows a reordering or a redistribution of the oxygen sublattice due to photoinduced hopping of oxygen atoms. Moreover, the dynamical changes in the CuO chains and their time scale are very similar to those observed in thermal relaxation of the PPC (see Ref. 3) and annealing effects on oxygen reordering,[16–18] and suggests an interpretation along the lines of the phenomenological "photoassisted oxygen ordering" model.[10–12] In this scenario, altering the order by photoactivated diffusion of chain-oxygen atoms, which increases the length of chain fragments, would result in a decreased defect density and an increased doping of superconducting CuO_2 planes, which is compatible with both transport and Raman-scattering experiments. However, in spite of the similarities between the two types of experiments, some important points should be clarified in order allow for Raman analysis of PPC and PPC-quenching effects: First, the microscopic mechanism of activation and deactivation of the defect-induced Raman

resonance needs to be at least qualitatively accounted for, and secondly, one needs to understand whether the dynamics of oxygen ordering can account for both photobleaching and quenching effects.

In this study, we utilized resonance Raman scattering, in combination with a tunable pumping excitation, as an *in situ* probe of structural changes in Y123 under illumination. This approach can potentially delineate electronic states with different energy depths, offering a unique tool to study metastability. Here, we show that two metastable states can be reversibly regulated by light. By measuring the photon energy dependence of this bidirectional photoswitching effect, and comparing with analogous data for the PPC/PPC-quenching effect, we show that the two phenomena have the same microscopic origin. Investigations of the photon polarization dependence allow us to conclusively link the photoinduced phenomena to the CuO chains in Y123 and to outline a microscopic interpretation in quantitative agreement with data.

II. EXPERIMENT

The samples were $YBa_2Cu_3O_{6+x}$ (Y123) single crystals grown by a flux method using a $BaZrO_3$ crucible.[19] After growth, the crystals were placed with Y123 buffer powder materials in a gas volumetric titration system that allows slow cooling over several weeks under variable oxygen partial pressures in order to provide the desired oxygen content. Data were obtained on twinned crystals with oxygen contents $x=0.6$, 0.72, and 0.8. Additional data were obtained on detwinned crystals with oxygen content $x=0.77$. The details of the structural properties are described elsewhere.[20]

The Raman and illumination measurements were made in a microscope/spectrometer setup modified so that two laser beams of different wavelengths could simultaneously illuminate the same area ($\sim 2\ \mu m^2$) on the sample, which was glued to the cold finger of a He microcryostat. The lines from Ar^+/Kr^+, dye, and Ti:sapphire lasers were used for illumination, and the 514.5 nm line from an Ar^+/Kr^+ laser was used for the Raman scattering measurements. The Raman spectra were measured in the backscattering geometry using a subtractive triple spectrometer (Jobin-Yvon Co. Ltd. T64000) equipped with a liquid-nitrogen-cooled charge-coupled-device detector. The spectra were obtained at 20 K, except for the study of temperature dependencies. To avoid heating and nonlinear effects at high incident laser powers, the power was usually 1 mW outside the cryostat which limits local heating to less than $\sim 10-20$ K, as confirmed by recording anti-Stokes spectra.

III. RESULTS AND DISCUSSION

A. Raman spectroscopic evidence for bidirectional photoswitching in Y123

Figure 1 shows photoinduced changes in the Raman spectra of a Y123 ($x=0.72$; $T_c=74$ K) single crystal with incident and scattered light polarized parallel to the CuO chains ($E\|b$) at $T=20$ K. The photoinduced structural modification is observed as a switching behavior of several resonance Raman modes (232, 263, 290, 305, and 592 cm^{-1}) associated with chain ends. Before photoexcitation with 514.5 nm light, the system is in the *unbleached* phase, characterized by intense resonantly enhanced phonon scattering from CuO chains, most notably for the 232 cm^{-1} mode. The intensity of this mode is proportional to threefold coordinated $Cu(1)_{chain}$ atoms [i.e., Cu(1) sites with only one oxygen vacancy neighbor in *long* CuO chains], and the observable is thus intimately linked to the detailed microscopic structure, i.e., oxygen vacancies in the CuO chains.[9–15] Visible illumination causes the CuO-chain resonance to almost completely *bleach* away, a behavior identical to the reported phonon bleaching.[9–14] This spectral change can be attributed to the photoinduced structural transition into the metastable ordered state characterized by a greatly reduced number of the threefold coordinated $Cu(1)_{chain}$.

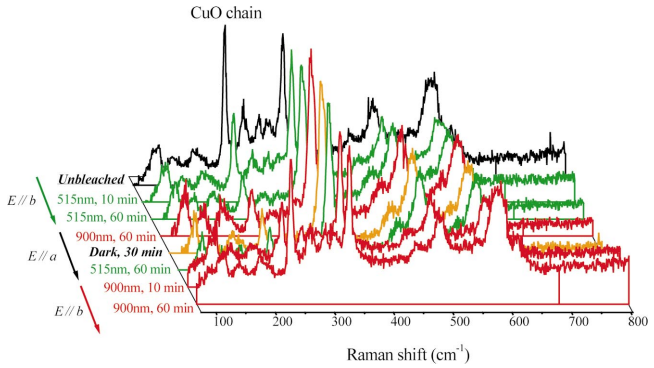

FIG. 1. (Color) Photoinduced changes in the Raman spectra of $YBa_2Cu_3O_{6.72}$ at 20 K with incident and scattered light polarized parallel to the CuO chains. Top spectrum is collected during the first 10 s of illumination with 514.5 nm light ($E\|b$). After 1 h of irradiation with 514.5 nm light, the photoinduced changes are then monitored during alternating cycles induced by different illumination wavelengths and polarizations. The time evolution of the 232 cm^{-1} chain-end phonon intensity under illumination can be followed in Fig. 2(a).

After 1 h of irradiation with 514.5 nm light, when the phonon line has bleached to one-quarter of the original intensity, the time evolution of the defect-induced phonon intensity is followed during alternating illumination cycles using different wavelengths and polarizations at $T=20$ K. The intensity is monitored at sequential time intervals by very short measurements using 514.5 nm Raman excitation. We found that the photoinduced (*bleached*) state is *quenched* by the chain-polarized NIR light. The time evolution of the 232 cm^{-1} phonon intensity under illumination can be followed in Fig. 2. A comparison of the upper and lower panels of Fig. 2 shows that the peak intensity is almost completely recovered ("*unbleached*") when the NIR light is polarized along the CuO chains ($E\|b$) while polarization across the chains ($E\|a$) has no effect at all. Note that this result is unaffected by the twinning of the single crystal: the strict polarization dependence of the observable (the chain-end phonons) guarantees that only twin domains oriented parallel to the probe-beam $\boldsymbol{E}$-field are sampled. No thermal relaxation of the bleached state is seen during the following 30 min in the dark, and the continued bleaching/unbleaching

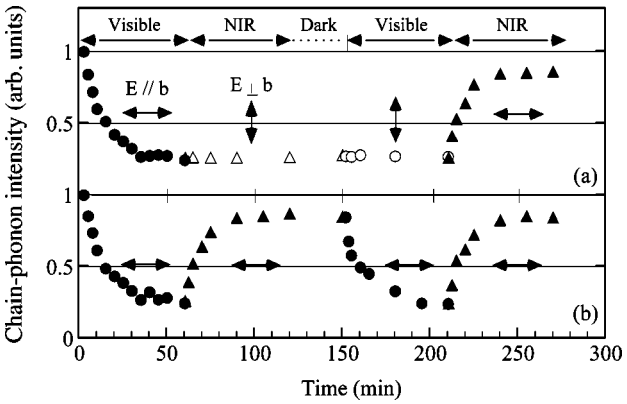

FIG. 2. Intensity of the 232 cm^{-1} chain-end Raman line during alternating cycles of photoinduced bleaching and unbleaching induced by different illumination wavelengths at $T=20$ K. The vertical and horizontal arrows denote light polarized parallel and perpendicular to the CuO chains, respectively.

cycles demonstrate that the photoswitching effect is fully reversible and repeatable below room temperature.

Figure 3 shows the unbleaching effect for various NIR laser intensities at $T=20$ K. As shown in the inset, the data can be rescaled with the cumulative photon dose, which together with the polarization sensitivity in Fig. 2 demonstrates that the phenomenon is a true; i.e., a nonthermal, photoinduced effect. Further, the dependence on cumulative photon dose follows a stretched-exponential Kohlrausch's law,[4] as is also the case for the phonon bleaching effect[10] and the PPC and PPC-quenching phenomena.[3,6] The photoswitching was found in all investigated samples with different oxygen contents ($x=0.6-0.8$), but with the largest absolute change in intensities of the chain-end modes occurring in the $YBa_2Cu_3O_{6.72}$ sample.

Figure 4 shows the bleaching and unbleaching efficiencies as a function of photon energy at $T=20$ K. The photoswitching phenomenon does not require any unique illumination wavelengths, as can be seen from the spectral efficiency

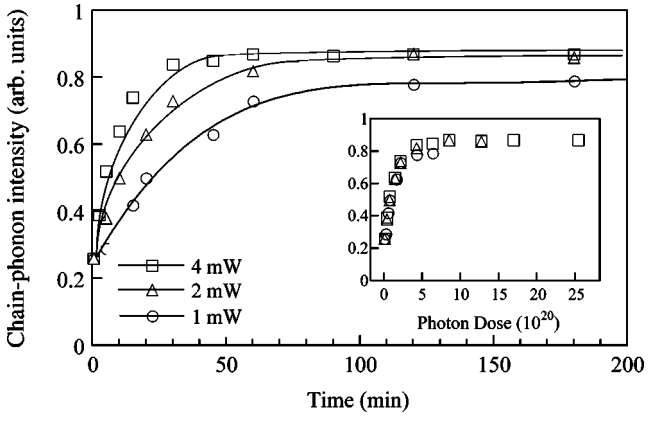

FIG. 3. Time dependence of the 232 cm^{-1} chain-end Raman line intensity under illumination with 900 nm NIR light of different powers. Inset shows the unbleaching efficiency normalized to cumulative photon dose at $T=20$ K. The dashed lines are guides to the eye.

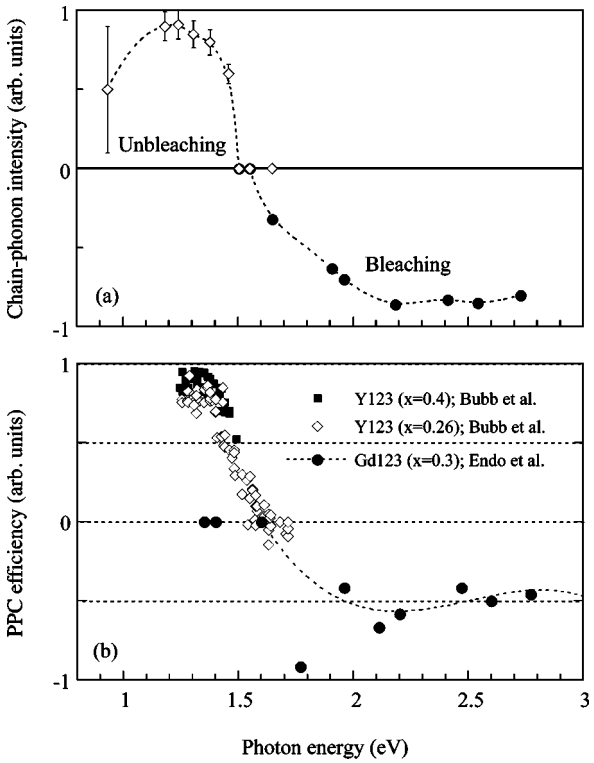

FIG. 4. (a) Bleaching and unbleaching efficiency as a function of photon energy. Data were obtained at different wavelengths but at the same photon density level (10^{21} photons/cm^2). (b) Spectral efficiency of PPC and PPC quenching from Refs. 21 and 6.

curves in Fig. 4(a). Both the bleaching and the unbleaching efficiency exhibit plateaus (at around $\hbar\omega > 2.2$ eV and $\hbar\omega < 1.3$ eV, respectively) and a broad transitional region centered at a crossover photon energy of around 1.6 eV. The data in Fig. 4(a) were acquired with the same cumulative photon dose irrespective of wavelength (1 h illumination at 10^{21} photons/cm^2). The nearly equal spectral efficiencies in the plateau regions thus means that it takes approximately the same number of photons to go from the bleached state to the unbleached state with, e.g., 900 nm NIR light, as it takes to go in the reverse direction with visible illumination. This indicates that the quantum efficiencies of the bleaching and the unbleaching processes are more or less the same. In Fig. 4(b) we have replotted previously published spectral efficiencies for the PPC effect[6,21] as a comparison to Fig. 4(a). It is clear that the datasets are very similar; e.g., the PPC-quenching efficiency reported by Bubb *et al.*[6] vanishes around 1.6 eV, which equals the bleaching/unbleaching crossover energy in Fig. 4(a). Together with the similarities in the thermal relaxation process and the temporal behavior noted above, Fig. 4 constitutes experimental evidence for a common microscopic mechanism behind the photoinduced effects observed by Raman spectroscopy and transport measurements.

B. Model for the photoswitching and possible connection to the persistent photoconductivity

We now consider the origin of the photoswitching phenomenon. As noted in the introductory paragraph, the

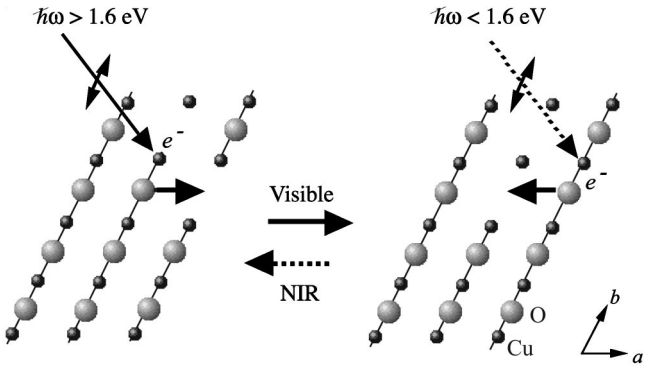

FIG. 5. Schematic illustration of the proposed model for reversible photoswitching of structural and transport properties in Y123. Chain-polarized visible light breaks short nondoping chain fragments and some oxygen recombine and form longer chain fragments, acting as dopants, thereby reducing the number of chain ends (A→B). These chain-fragments are broken by chain-polarized NIR light (B→A).

"oxygen-ordering model" has provided a phenomenological rationale for interpretations of the photoinduced metastability in Y123. However, the microscopic mechanism has remained obscure. We believe that the data presented here put severe constraints on a microscopic model. Most important, the exclusively *y*-polarized character of both the primary photo effect (phonon bleaching, PPC) and the reverse process (unbleaching, PPC quenching) strongly indicates that the optical transitions involved are directed along the CuO chains. Transitions within or between the tetragonal elements of the Y123 structure, such as the CuO_2 planes or the CuO_2 dumbbells, can be ruled out. Moreover, the similar quantum efficiencies of the primary and reverse processes indicate that only one type of transition is involved. We propose that this transition is dipole allowed and has a substantial O_{chain}-to-Cu_{chain} charge-transfer character of the type

$$\cdots Cu^{2+}O^{2-}\cdots + \hbar\omega \rightarrow \cdots Cu^{+}O^{-}\cdots . \tag{1}$$

Both lattice dynamical calculations and experimental observations show that the CuO chains are only marginally stable against oxygen displacements in the *a* direction.[22,23] A charge transfer excitation will decrease the Cu—O Coulomb attraction, and therefore lower the already small energy barrier against oxygen movement out of the chains. Chain-polarized visible illumination will therefore promote chain-oxygen diffusion. The experimental observations described above can be understood if we assume that the charge-transfer excitation energy *decreases with increasing chain length L*. A schematic illustration of the proposed model for reversible photoswitching in Y123 is shown in Fig. 5. If this is the case, then long-wavelength (NIR) and short-wavelength (visible) illumination will tend to destabilize long chains and short chains, respectively. Oxygen ions that are kicked out of short chains by visible light will be able to recombine into longer chains, causing a net reduction in the chain-end density (phonon bleaching effect) and a net increase of the CuO_2 plane hole doping (PPC effect). The reverse effects would occur if oxygen ions were kicked out of long chains by NIR light.

In order to get a rough idea of how the chain length could influence the relevant electronic transitions, we use a simplified version of the "particle-in-a-box" problem of basic quantum mechanics, which has been used successfully to explain the variation of absorption band position with chain length in conjugated dye molecules.[24] We consider the chain as a potential well of length $L=nb$ populated with N electrons, where $b\approx 3.9$ Å is the lattice parameter and n is the number of chain segments. The excitation energy for the dipole transition from the highest occupied level to the lowest unoccupied level is then

$$\hbar\omega = \frac{\hbar^2\pi^2}{2m_eL^2}(1+N), \tag{2}$$

which confirm the aforementioned inverse dependence on chain length L. Interestingly, if we assume that a chain segment contributes two "free" electrons, i.e., $N=2n$, we obtain

$$\hbar\omega \approx \left[\frac{1}{n^2}+\frac{2}{n}\right]2.60\ \text{eV}, \tag{3}$$

i.e., the correct energy range for optical transitions in short chains. Note that Eq. (3) for $n=4$ yields $\hbar\omega\approx 1.5$ eV, which matches the crossover photon energy between PPC and PPC quenching as well as Raman line bleaching and unbleaching shown in Fig. 4 surprisingly well.

In Eq. (1) and Fig. 4 we have used the $3d^9$ and $3d^{10}$ L states of a neutral CuO molecule to indicate the ground and optically excited states, respectively.[22] The real states of a CuO chain are of course mixed, leading to noninteger ionic charges and highly dispersive energy bands for the infinite chain. However, the simple interpretation suggested above can be compared to both theoretical and experimental data on the optical conductivity,[25,26] which in addition provides support for the charge-transfer character of the optical transition of small CuO-chain clusters. Based on a *t-J* model, Aligia *et al.* found several low-frequency ($\hbar\omega=1-4$ eV) excitonic conductivity peaks, in which a hole of mainly Cu character is transferred to an oxygen.[25] The positions of these charge-transfer excitations vary strongly with doping and, most important, this study reveals a chain length dependence of the lowest lying excitation in long chains according to $\hbar\omega\propto 1/(n+1)$, where n is the number of chain oxygen ions in an isolated chain fragment. In a very recent study on reflectance-anisotropy spectra,[26] Bruchhausen *et al.* reported that well-resolved spectral features at 2.2 and 4.1 eV either bleached or enhanced on photoexcitation pararell to the Cu(1)—O(1) chains, a behavior similar to that observed in phonon bleaching. They ascribed these changes to the time evolution of the number of Cu_{chain} atoms belonging either to $O(1)—Cu—O(4)_2$ short chain fragments with threefold coordination (transition at 2.2 eV) and to isolated $Cu(1)—O(4)_2$ clusters with twofold coordination (transitions at 4.1 eV). If we use the relationship $\hbar\omega\propto 1/(n+1)$ also for short chains and our results, and assume that $n=1$ [isolated $Cu(1)—O(4)_2$ chains] corresponds to $\hbar\omega\approx 4.5$ eV, the highest energy reported for the PPC efficiency,[21] then the

low-energy flank in the PPC and phonon-bleaching efficiencies in Fig. 3 ($\hbar\omega \approx 1.6-2$ eV) would correspond to $n \approx 3,4$ [transition involving electronic states of Cu(1) in short chain fragments with small clusters, Cu_3O_8, Cu_4O_{11}], while the optimal wavelengths of the PPC-quenching and phonon-unbleaching efficiency ($\hbar\omega \approx 1.3$ eV) would correspond to $n \approx 5$ (Cu_5O_{14} clusters). It is generally believed that chain fragments with lengths below a critical one ($L_c < 4$) do not contribute to the intrinsic chain-to-plane doping mechanism in Y123.[27] This suggests a coherent interpretation of the PPC and PPC-quenching phenomena; namely, that transitions immediately above and below the crossover energy ($\hbar\omega = 1.6$ eV) in Fig. 3 are charge-transfer excitations that destabilize the longest nondonor and shortest donor chain fragments, respectively.

C. Origin of the chain-polarized Raman resonance

Finally, we briefly discuss the origin of the chain-polarized Raman resonance in Fig. 1. This is a matter of continued debate,[9–12] and is also of practical interest as the resonance enhancement severely complicates the suggested use of the chain-end phonon *intensity* as a simple measure of the actual chain-end *density*.[11] Of the proposed mechanisms, electric-quadrupole/magnetic-dipole transitions in infinite chains[9] and transitions within special oxygen superstructures[12] have been ruled out due to the resonance dependence on oxygen content and temperature, respectively.[10,12] An origin related to vacancy states in long CuO chains[9,10] remains a possibility. Returning to the data in Fig. 4, we see that the resonance profile coincides with the low-energy flank of the PPC and phonon-bleaching efficiency curves. This indicates that the aforementioned charge-transfer transition in the longest nondonor chain fragments takes part in the resonance Raman process. In the case of randomly distributed oxygen vacancies, the density of fragments of length L scales as $(x-1)^2 x^L$, which is maximal at $x = 2/3$ for $L_c = 4$. This agrees well with the intensity maximum of the chain-end phonons at around $x = 0.7$.[10,12] It would be interesting to investigate this possibility through *ab initio* cluster calculations including phonon degrees of freedom. Additionally, such calculations could possibly resolve fundamental questions regarding the stability of small chain fragments in various optically excited states.

IV. SUMMARY

We have shown that the intensity of resonant chain-end phonons in Y123 can be regulated by light polarized parallel to the CuO chains. Visible light ($\hbar\omega > 1.6$ eV) bleaches the phonons, while the reverse effect occurs for near-infrared illumination ($\hbar\omega < 1.6$ eV). The spectral, thermal, and temporal responses are essentially identical and analogous to the persistent photoconductivity effect in Y123. We suggest a common microscopic mechanism based on charge-transfer-type chain-polarized optical transitions for which the excitation energy varies inversely with chain length and for which the excited state is unstable against oxygen movement in the *a* direction. Depending on the incident photon energy, illumination therefore destabilizes different CuO chains and allows for the buildup of thermally inaccessible chain-length distributions with altered macroscopic optical and transport properties.

ACKNOWLEDGMENTS

This work was financially supported by the Swedish Superconductivity Consortium. M. O. acknowledges the financial support of PRESTO, Japan Science and Technology Agency (JST).

*Also at PRESTO, Japan Science and Technology Agency; electronic address: osada.minoru@nims.go.jp

†Present address: Permascand AB, Box 42, SE-84010 Ljungaverk, Sweden

[1] V. I. Kudinov, A. I. Kirilyuk, N. M. Kreines, R. Laiho, and E. Lähderanta, Phys. Lett. A **151**, 358 (1990).

[2] G. Nieva, E. Osquiguil, J. Guimpel, M. Maenhoudt, B. Wuyts, Y. Bruynseraede, M. B. Maple, and I. K. Schuller, Appl. Phys. Lett. **60**, 2159 (1992).

[3] V. I. Kudinov, I. L. Chaplygin, A. I. Kirilyuk, N. M. Kreines, R. Laiho, E. Lähderanta, and C. Ayache, Phys. Rev. B **47**, 9017 (1993).

[4] The variation of photoconductivity $R(t)$ is given by the stretched-exponential Kohlrausch law [G. Williams *et al.*, Trans. Faraday Soc. **66**, 80 (1970)], $R(t) = R_0[1 - \exp - (t/\tau)^{\beta}]$, where t is time, τ is a time constant, and the exponent β lies in the range 0 to 1, depending on light intensity and temperature. This law is a signature of a microscopic distribution of energy barriers or a hierarchical relaxation process.

[5] D. C. Chew, J. F. Federici, J. Gutierrez-Solona, G. Molina, W. Savin, and W. Wilber, Appl. Phys. Lett. **69**, 3260 (1996).

[6] D. M. Bubb, J. F. Federici, S. C. Tidrow, W. Wilber, J. Kim, and A. Piqué, Phys. Rev. B **60**, 6827 (1999).

[7] E. Osquiguil, M. Maenhoudt, B. Wuyts, Y. Bruynseraede, D. Lederman, and I. K. Schuller, Phys. Rev. B **49**, 3675 (1994).

[8] J. F. Federici, D. Chew, B. Welker, W. Savin, J. Gutierrez-Solana, T. Fink, and W. Wilber, Phys. Rev. B **52**, 15592 (1995).

[9] D. R. Wake, F. Slakey, M. V. Klein, J. P. Rice, and D. M. Ginsberg, Phys. Rev. Lett. **67**, 3728 (1991).

[10] M. Käll, M. Osada, M. Kakihana, L. Börjesson, T. Frello, J. Madsen, N. H. Andersen, R. Liang, P. Dosanjh, and W. N. Hardy, Phys. Rev. B **57**, R14072 (1998).

[11] A. Fainstein, P. Etchegoin, and J. Guimpel, Phys. Rev. B **58**, 9433 (1998).

[12] A. G. Panfilov, A. I. Rykov, S. Tajima, and A. Yamanaka, Phys. Rev. B **58**, 12459 (1998).

[13] A. Fainstein, B. Maiorov, J. Guimpel, G. Nieva, and E. Osquiguil, Phys. Rev. B **61**, 4298 (2000).

[14] S. Bahrs, A. R. Goñi, C. Thomsen, B. Maiorov, G. Nieva, and A. Fainstein, Phys. Rev. B **65**, 024522 (2002).

[15] V. G. Ivanov, M. N. Iliev, and C. Thomsen, Phys. Rev. B **52**, 13 652 (1995).
[16] B. W. Veal, A. P. Paulikas, H. You, H. Shi, Y. Fang, and J. W. Downey, Phys. Rev. B **42**, 6305 (1990).
[17] A. A. Maksimov, D. A. Pronin, S. V. Zaitsev, I. I. Tartakovskii, G. Blumberg, M. V. Klein, M. Karlow, S. L. Cooper, A. P. Paulikas, and B. W. Veal, Phys. Rev. B **54**, R6901 (1996).
[18] A. A. Maksimov, D. A. Pronin, S. V. Zaitsev, I. I. Tartakovskii, M. V. Klein, and B. W. Veal, J. Exp. Theor. Phys. **89**, 366 (1999).
[19] R. Liang, P. Dosanjh, D. A. Bonn, D. J. Baar, J. F. Carolan, and W. N. Hardy, Physica C **195**, 51 (1992).
[20] N. H. Andersen, M. von Zimmermann, T. Frello, M. Käll, D. Mønster, P.-A. Lindgård, J. Madsen, T. Niemöller, H. F. Poulsen, O. Schmidt, J. R. Schneider, Th. Wolf, P. Dosanjh, R. Liang, and W. N. Hardy, Physica C **317–318**, 259 (1999).
[21] T. Endo, A. Hoffmann, J. Santamaria, and I. K. Schuller, Phys. Rev. B **54**, R3750 (1996).
[22] For a review, see W. E. Pickett, Rev. Mod. Phys. **61**, 433 (1989).
[23] J. D. Jorgensen, S. Pei, P. Lightfoot, H. Shi, A. P. Paulikas, and B. W. Veal, Physica C **167**, 571 (1990).
[24] F. P. Schöafer, in *Topics in Applied Physics Vol. 1: Dye Lasers*, edited by F. P. Schöafer (Springer-Verlag, Berlin, 1990).
[25] A. A. Aligia, E. R. Gagliano, and P. Varius, Phys. Rev. B **52**, 13601 (1995).
[26] A. Bruchhausen, S. Bahrs, K. Fleischer, A. R. Goñi, A. Fainstein, G. Nieva, A. A. Aligia, W. Richter, and C. Thomsen, Phys. Rev. B **69**, 224508 (2004).
[27] J. Zaanen, A. T. Paxton, O. Jepsen, and O. K. Andersen, Phys. Rev. Lett. **60**, 2685 (1988).